Journal of Manufacturing Processes
Vol. 4/No. 1
2002

Existence and Effects of Overlap Factors Greater than Unity and Less than Zero

William J. Endres, Dept. of Mechanical Engineering and Applied Mechanics, University of Michigan, Ann Arbor, Michigan, USA*
O. Burak Ozdoganlar, Dept. of Mechanical and Industrial Engineering, University of Illinois at Urbana-Champaign, Urbana, Illinois, USA†

Abstract

A geometric model of the dynamic chip area for processes that employ corner-radiused tools is used to show how the resulting mathematical expressions for overlap factor lead to values outside the traditional range of zero to unity. The mathematical expressions are geometrically interpreted through schematics of the process geometry. The orthogonal cutting stability solution shows that results are identical for positive and negative overlap factors of the same magnitude. The effects of overlap factor outside the traditional range are shown; however, it is shown that coupling overlap factor to other directional factors, through the depth of cut (the dependent variable), makes it impossible to interpret stability results based on the overlap factor concept alone. Specific examples show that while overlap factor often exceeds unity for corner-radiused tools, reaching extreme values that approach infinity does not seem to occur due to the strong dependence on the depth of cut—the dependent variable of the stability analysis.

Keywords: *Machining Stability, Overlap Factor, Turning, Chatter*

Introduction

One of the major considerations in determining the stability behavior of a machining operation is the regenerative effect. This effect arises because at any instant in time a tooth is removing a surface machined by the previous tooth pass. Making use of the idea of Merchant (1944) and others that the machining force is proportional to the uncut chip area, fundamental theories of machining stability began to emerge in the 1950s. The early theoretical developments focused on the straight-edged orthogonal cutting process. This process is the type achieved in tube-end turning and had been the focus of most of the fundamental cutting mechanics work to that date. Not long after the early explanations of the regeneration concept offered by Tobias and Fishwick (1958), it was recognized that the orthogonal cutting stability theories were limited in their direct extension to more commonly used processes, such as turning, milling, and grinding.

Toward extending the basic theories to processes of industrial interest, a parameter called *overlap factor* was conceived (Tobias and Fishwick 1958, Gurney and Tobias 1961, Merritt 1965, Sweeney and Tobias 1969, Moriwaki and Iwata 1976, Srinivasan and Nachtigal 1978, Nigm 1981). The overlap factor was introduced to reflect the fact that a cutting tooth may only partially "overlap" the surface produced by the preceding tooth pass. Those working on the problem at the time proposed that while the overlap factor would be unity for the orthogonal cutting process they were studying, it would take on values of zero for thread cutting and something between zero and unity for other processes.

It is important to understand that overlap factor is not a physically controllable parameter. It is a parameter introduced to extend the mathematics. For the most part, researchers have not known what the overlap factor values should be for specific processes, not to mention how overlap factor would relate to the process parameters that are introduced by the geometry of other processes. As such, overlap factor has remained a mathematical concept that has little physical connection to the real processes that initiated its introduction. Nevertheless, the early efforts to make the theory extendible by introducing an overlap factor have made the theory more useful in the long run.

Introducing overlap factor creates some difficulty in computationally evaluating an analytical stability solution. Some of the early works employed graphical techniques (Gurney and Tobias 1961, Merritt 1965, Sweeney and Tobias 1969) where this complication was not as much of a hindrance. Since then, many researchers have discussed overlap factor and

---

*Now with the Dept. of Mechanical Engineering-Engineering Mechanics, Michigan Technological University, Houghton, Michigan, USA.

†Now with the Structural Dynamics and Smart Systems organization at Sandia National Laboratories.

This paper is an original work and has not been previously published except in the *Transactions of NAMRI/SME,* Vol. XXIX, 2001.

included it in the derivation of their solution. While many subsequently set it equal to unity to facilitate computations, a few researchers (e.g., Nigm 1981, Jensen and Shin 1997) have performed their computations for non-unity (constant) overlap factors in order to study its effects. However, little has been done to actually model the overlap factor as a function of process parameters like depth of cut, feed, and edge profile shape. Despite the common use of corner-radiused tools in most turning, boring, and face milling operations, only a few studies of overlap factor for the turning process can be found in the literature (Srinivasan and Nachtigal 1978, Moriwaki and Iwata 1976).

The work presented here arose from the analytical treatment of the turning stability problem when corner-radiused tools are used and the structural dynamics are not assumed to be solely in either the feed direction or the depth-of-cut direction. The work of the authors began by formulating an analytical expression for chip area variation in the presence of both feed and depth variations from one tooth pass to the next (Ozdoganlar and Endres 2000). That effort laid the foundation for a stability solution (Ozdoganlar and Endres 1998) that accounts for the geometrical effects of corner radius, lead angle, feed, depth of cut, and orientation of the mode in the feed-depth plane. In fact, it is the mode orientation that makes the problem very interesting and leads to the new finding presented here—that overlap factor may take on any value, not only those between zero and unity. The latter has been the presumption since the 1950s when overlap factor and its concept were first introduced.

Dynamic Process Force for a Corner-Radiused Tool

The development of an analytical representation of the process force acting on a corner-radiused tool that experiences depth-direction vibration has been well documented in a previous work by the authors (Ozdoganlar and Endres 1998, 2000). The presence of a corner radius and lead angle is explicitly accounted for in the process force expressions. Their effects become particularly important when the structural dynamics of interest introduce vibration in the depth-of-cut direction, not just the feed direction. A brief review of how the overlap factor expression was derived is presented here to facilitate later discussion.

The process geometry of interest is shown in *Figure 1*, where r_ε is the corner radius, ψ_r is the lead angle, f_t is the feed per tooth, and d_e is the equilibrium depth of cut. These are the four geometric parameters that define the profile shapes and sizes and their relative equilibrium positions. The figure shows two subsequent edge profiles of a corner-radiused tool that possesses single-dimensional dominant dynamics with displacement $q(t)$. The direction of the q mode is defined relative to the feed direction by the mode orientation angle θ. The process force in this plane, the thrust force component F_T, is often modeled to be proportional to the chip area and oriented at an equivalent lead angle $\overline{\psi}$. Because it is the overlap factor that is of interest at this point, and because the overlap factor is a parameter within the chip area expression, the discussion here will take place at the level of chip area, not the process force. Issues related to the force-model level will be noted later.

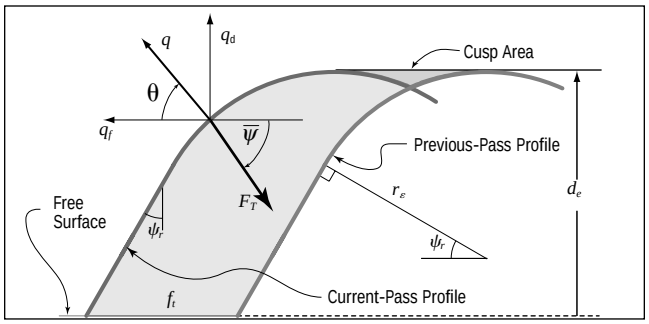

Figure 1
Process Geometry Showing Mode Orientation

Of interest in the stability problem is the *dynamic* force. The dynamic force is proportional to the *dynamic* chip area, keeping in mind that other process dynamics such as process damping are not considered here. The dynamic chip area for orthogonal cutting is historically written as

$$\Delta a(t) = d \cdot \Delta f(t) = d\left[q_f(t) - \mu q_f\left(t - T_t\right)\right] \quad (1)$$

where $\Delta f(t)$ is the dynamic variation in the feed, d is the depth of cut, $q_f(t)$ is the displacement in the feed direction, and T_t is the tooth period—the regenerative delay. In past works on turning stability, where it is assumed there is no depth-direction component of vibration, this formulation is sufficient as it captures the full effect of vibration in this plane, $q_f(t)$. This would correspond to θ, as shown in *Figure 1*, being zero.

When the dynamics of interest are oriented in any direction other than $\theta = 0$, depth-direction vibration occurs and a more comprehensive form of the dynamic chip area is needed, such as

$$\Delta a(t) = b_f\left[q_f(t) - \mu_f q_f(t - T_t)\right] + b_d\left[q_d(t) - \mu_d q_d(t - T_t)\right] \quad (2)$$

This expression accounts for vibrations in both *process coordinates—q_d* in the depth direction and q_f. Associated with each coordinate is an overlap factor, μ_d or μ_f. The dynamic chip area can also be written in the traditional overlap form of final interest, that relating to the q-direction:

$$\Delta a(t) = b_q\left[q(t) - \mu_q q(t - T_t)\right] \quad (3)$$

Equating Eqs. (2) and (3) and introducing the relations of the feed and depth directions to the q direction (a rotational transformation) allows μ_q to be written as

$$\mu_q = \frac{b_f\mu_f\cos\theta + b_d\mu_d\sin\theta}{b_f\cos\theta + b_d\sin\theta} \quad (4)$$

This is the overlap factor of ultimate interest as it is the one that corresponds to the actual dynamic mode. The parameters b_f, b_d, μ_f, and μ_d are derived from the analytical representation of the chip area.

Derivation of Overlap Factor Expressions

Deriving expressions for b_f, b_d, μ_f, and μ_d evolves from the first step of an analytic formulation for chip area under the influence of depth-direction variation (Ozdoganlar and Endres 2000). The chip area expressions derived there are highly nonlinear in Δf, Δd_0, and Δd_1, where Δd_0 and Δd_1 are variations in depth of cut for the current and previous tooth passes, respectively. These variables are related to the displacement state variables, through the variations in feed and depth of cut $q_f(t)$ and $q_d(t)$ of Eq. (2), as

$$\Delta f = q_f(t) - q_f(t - T_t), \quad \Delta d_0 = q_d(t), \quad \Delta d_1 = q_d(t - T_t) \quad (5)$$

The nonlinear chip area expressions were then linearized in a subsequent work (Ozdoganlar and Endres 1998) for use in deriving an analytical stability solution. Introducing the relations of Eq. (5) and equating the dynamic part of the linearized chip area expressions to the form of Eq. (2) resulted in fairly simple expressions for b_f, b_d, μ_f, and μ_d. There are two sets of results, one for small depths of cut that are less than the transition depth $d_t = r_\varepsilon(1 - \sin\psi_r)$ and one for large depths of cut that are greater than d_t. Subscripts '*S*' and '*L*' are used to differentiate the two results as needed. The details of these derivations can be found in the two cited references; however, for discussion purposes, the end results for the large-depth case are provided here:

$$b_{f_L} = d_e - r_\varepsilon + \sqrt{r_\varepsilon^2 - \frac{f_t^2}{4}}, \quad b_{d_L} = d_e\tan\psi_r + \frac{r_\varepsilon(1 - \sin\psi_r)}{\cos\psi_r} + \frac{f_t}{2} \quad (6)$$

$$\mu_{f_L} = 1, \quad \mu_{d_L} = \frac{d_e\tan\psi_r + \dfrac{r_\varepsilon(1 - \sin\psi_r)}{\cos\psi_r} - \dfrac{f_t}{2}}{d_e\tan\psi_r + \dfrac{r_\varepsilon(1 - \sin\psi_r)}{\cos\psi_r} + \dfrac{f_t}{2}} \quad (7)$$

As a side note, $b_{f_S} = b_{f_L} = b_f$ and $\mu_{f_S} = \mu_{f_L} = \mu_f = 1$, always; this result will be interpreted later. Substitution of the b and μ expressions into Eq. (4) simplifies to

$$\mu_{q_L} = \frac{b_f\cos\theta + \left(d_e\tan\psi_r + \dfrac{r_\varepsilon(1 - \sin\psi_r)}{\cos\psi_r} - \dfrac{f_t}{2}\right)\sin\theta}{b_f\cos\theta + \left(d_e\tan\psi_r + \dfrac{r_\varepsilon(1 - \sin\psi_r)}{\cos\psi_r} + \dfrac{f_t}{2}\right)\sin\theta} \quad (8)$$

Special Overlap Factor Values

Equation (8) clearly highlights that the deviation of μ_q from unity is driven by a single flip in sign, in one term, from the numerator to the denominator. The $f_t/2$ term being subtracted in the numerator provides a feel for the traditional interpretation that the numerator would be less than the denominator, yielding an overlap factor less than unity. While it is clear that the overlap factor approaches the often-assumed value of unity as the feed approaches zero, the more interesting and substantial effects come from the other parameters, in particular the mode orientation angle θ. In other words, while the feed can drive μ_q down from unity, that can occur only when $\sin\theta$ is nonzero, unlike the often-studied case of feed-direction dynamics in which $\sin\theta = 0$.

In fact, considering θ, it is conceivable that μ_q could not only reach the extreme of zero, when the numerator equals zero, but could also approach infinity when the denominator tends to zero, and could be negative as well.

Without addressing any of the individual parameters other than mode orientation angle, one may note that the overlap factor can be written generically as

$$\mu_q = \frac{b_f \cos\theta + (b_d - f_t)\sin\theta}{b_f \cos\theta + b_d \sin\theta} \tag{9}$$

Given this, the following two situations could arise:

$$\mu_q = 0 \text{ when } b_f \cos\theta + (b_d - f_t)\sin\theta = 0$$

$$\text{or } \tan\theta = \frac{-b_f}{b_d - f_t}$$

and

$$\mu_q \to \infty \text{ as } b_f \cos\theta + b_d \sin\theta \to 0$$

$$\text{or } \tan\theta \to \frac{-b_f}{b_d}$$

On the one hand, if these situations were to occur only when the other parameters take on physically unrealizable values, for example only for negative depths of cut, then there would be nothing of physical interest to consider. However, because $\sin\theta$ and $\cos\theta$ vary from -1 to +1 and furthermore they can have either the same or opposite sign for a given θ, each of these situations must occur irrespective of the signs and relative magnitudes of b_f and b_d, in other words, irrespective of the signs and magnitudes of the other process parameters. The figures discussed in the next section confirm this fact. The mode orientation angle at which overlap factor approaches infinity will be denoted θ_∞.

Overlap Factor Values for Corner-Radiused Tools

Moriwaki and Iwata (1976) expressed the overlap factor for corner-radiused tooling as the ratio of the width of cut of the previous-pass profile to that of the current-pass profile. It was stated that the overlap factor thus calculated would be bounded between zero and unity. Their efforts focused on the relative profiles while the dynamic mode was considered to lie solely in the depth direction. Srinivasan and Nachtigal (1978) considered direction-specific overlap factors (μ_f and μ_d) and recognized that the feed-direction overlap factor is always unity for a traverse turning operation. These considerations are in agreement with the findings presented here. However, the depth-direction overlap factor derived in their study is independent of the corner radius. Like Moriwaki and Iwata (1976), they too departed from the usual feed-direction dynamics by considering the dynamics to be in the depth direction. Careful study of their formulation suggests that they too would have found overlap factors outside the traditional range [0, 1] if they had transformed their equation of motion into a particular mode orientation other than the depth-direction only.

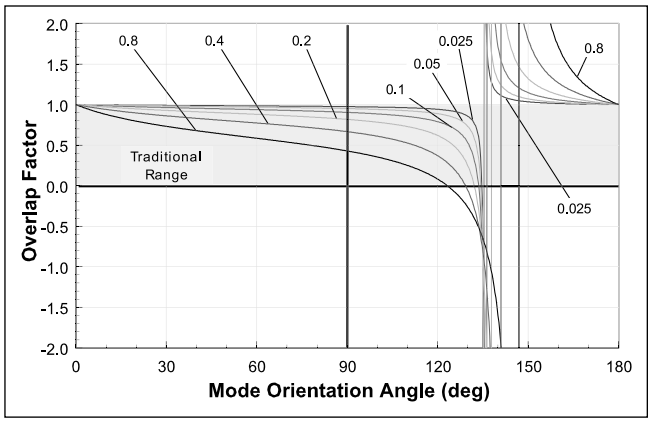

Figure 2
Overlap Factor vs. Mode Orientation Angle for Six Different Nondimensional Feeds per Tooth (F_t) at D_e = 1 and ψ_r = 0°

Overlap Factor Variation with Process Variables

As the authors noted in a past work (Ozdoganlar and Endres 2000), any geometrical characteristic of the corner-radiused process geometry can be nondimensional by the corner radius. Therefore, Eq. (8) could have been written in terms of the nondimensional feed ($F_t = f_t/r_\varepsilon$) and depth ($D_e = d_e/r_\varepsilon$) with no mention of corner radius. This removes one (r_ε) of the five variables from the study, leaving the effects of feed, depth of cut, lead angle, and mode orientation angle to be explored. Note that in terms of defining the mode orientation, angles from 180° to 360° are equivalent to the range of 0° to 180°, and, therefore, would mirror the results shown in these figures.

Figure 2, as a general example, shows clearly how the overlap factor extends outside the shaded "traditional range" of zero to unity and how it can approach $\pm\infty$ (at θ_∞). The figure is intended to focus on the effects of feed, showing that feed has little effect on θ_∞, but strongly dictates the extent (by how

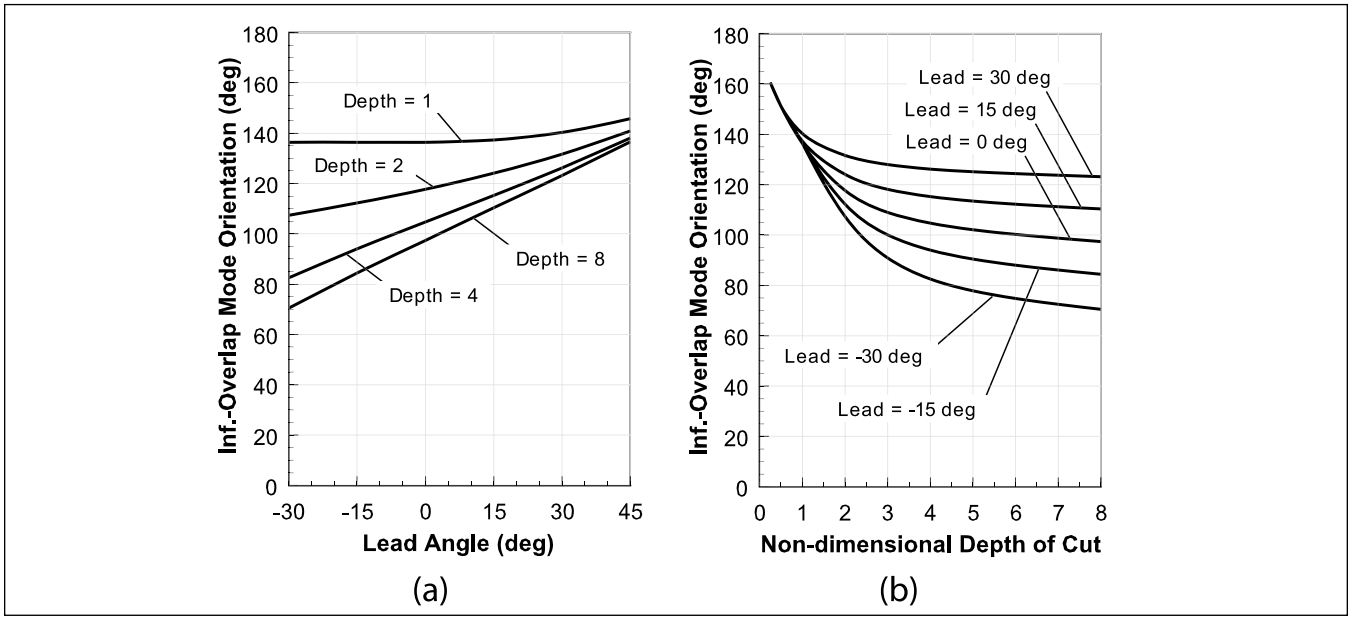

Figure 3
Variation in θ_∞ with Lead Angle and Nondimensional Depth of Cut for F_t = 0.1

much and over what range of θ) to which overlap factor deviates from unity. Large deviation from unity occurs over a large range of mode orientation angle, even at very practical levels of feed (20-40% of the corner radius).

In studying the effect of lead angle, some amount of cutting must occur on the lead edge for the lead angle to have any effect. This requires that the depth of cut be greater than $d_t = r_\varepsilon(1-\sin\psi_r)$. Therefore, a depth of twice the corner radius or greater is considered to assure that $d_e > d_t$ for any lead angle. The depth of cut and lead angle are found to mainly cause a shift in θ_∞ while having little effect on the extent of deviation from unity, which is the primary effect of feed. *Figure 3a* shows that the effect of lead angle is pronounced (greater slope) at larger depths, while *Figure 3b* shows that the effect of depth diminishes quickly and exponentially as depth increases. To summarize, the effect of lead angle on θ_∞ is greater at larger depths, but mainly only when the lead angle is on the smaller (becoming negative) side.

One might intuitively expect the aforementioned interaction effect of lead angle and depth of cut, that is, that the effect of lead angle would be stronger at larger depths of cut because a larger depth of cut increases the amount of cutting that occurs on the lead edge. However, the pronounced effect of lead angle at larger depths of cut occurs only for smaller (becoming negative) lead angles, which are, in fact, those where less cutting occurs on the lead edge while more cutting occurs on the corner radius. This counterintuitive twist occurs because the issue here is not only the extent of cutting on the lead edge, but also the location at which the lead edge intersects the free surface, as measured relative to the point where the edge profiles intersect at the tip of the cusp (see *Figure 1*). This issue is clarified in the geometric interpretation of the next subsection.

Interpretation of Extreme Values

The overlap factor solution presented here may be interpreted by showing graphically how the terms in the overlap factor expressions are affected by changes in the process geometry. Recall the physical meaning of overlap factor—the ratio, to the (current) width of cut, of the width of the undulated, previously cut surface that is participating in the current cut. These two quantities are, respectively, the numerator and denominator of Eq. (9). From a process modeling perspective, the widths of cut are usually considered to be the curvilinear distances measured along the portions of the edge profiles that bound the chip area. From a dynamics and overlap factor perspective, one must consider the *dynamic widths*. As concluded from this study, the dynamic widths are simply the lengths of the lines connecting the “ends” of the chip area, which are shown as dashed lines in *Figure 4*. The ends of the chip area are labeled in the figure, one being the intersection of the corner radii of the two tooth profiles (point *I*), and the other two correspond-

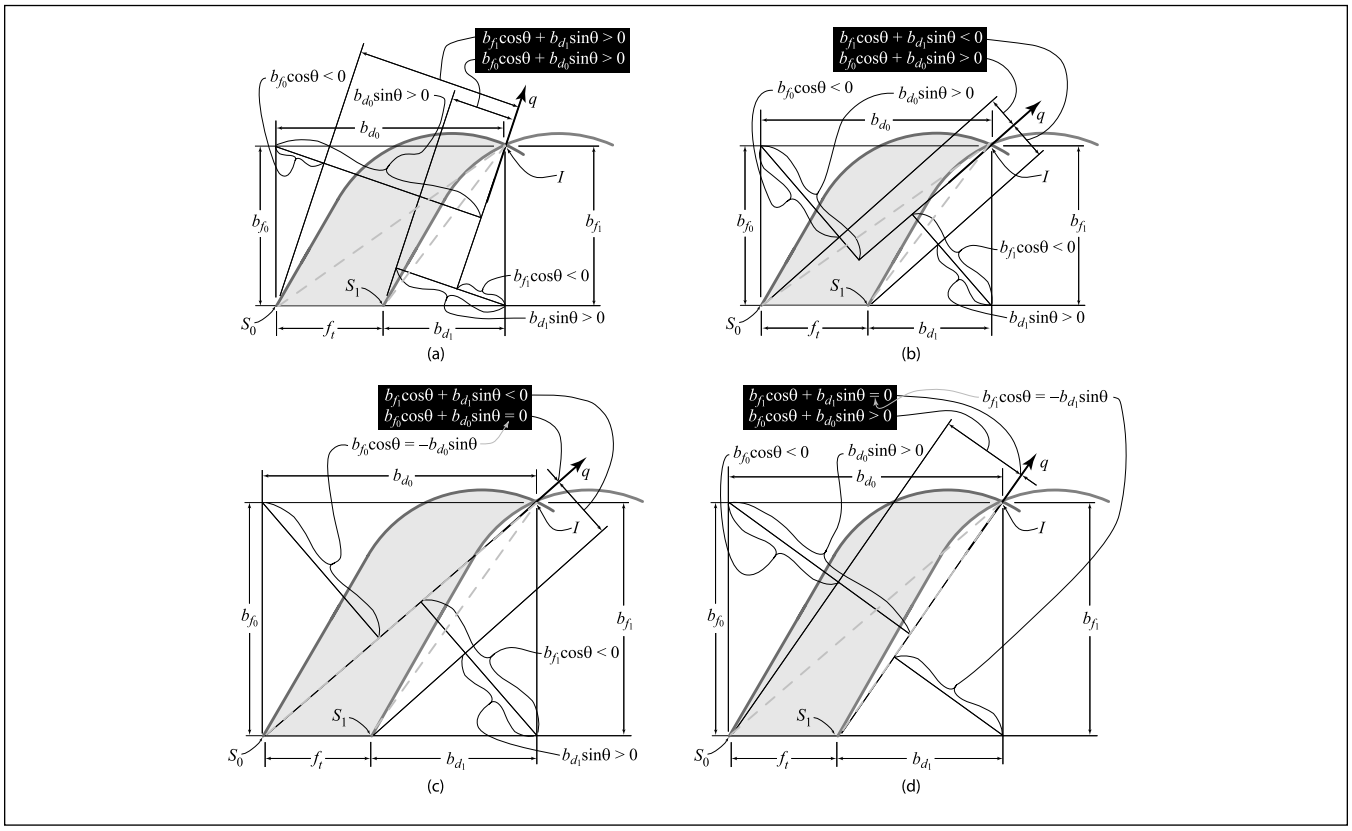

Figure 4
"Ends" of Chip Area and Their Projections that Result in μ_f and μ_d and in μ_q Being: (a) Positive, (b) Negative, (c) Infinite, and (d) Zero

ing to the intersection of each tooth profile with the free surface (S_0 and S_1). Here and to follow, the subscripts 0 and 1 refer to the current and previous tooth passes, respectively.

Once a particular direction is considered for an overlap factor, i.e., depth-direction (μ_d) or feed-direction (μ_f) or mode-direction (μ_q), the distances of interest are the projections of the dynamic widths onto the line normal to the direction of interest. For instance, for $\mu_d = b_d/(b_d - f_t)$, the projections are made onto the feed direction, as it is the normal to the direction of interest—the depth direction. These projections are shown in *Figure 4* as b_{d_0} (= b_d) and b_{d_1} (= $b_d - f_t$). For μ_q, the projections are made onto the line oriented at $\theta + \pi/2$. Therefore, μ_q [Eq. (9)] can be related to the process geometry of *Figure 4* in the following way. The numerator of Eq. (9) ($b_f\cos\theta + (b_d - f_t)\sin\theta$) is the sum of the projections, into the q-normal direction, of the *previous-pass* dynamic width having first been projected into the feed ($b_{f_1} = b_f$) and depth ($b_{d_1} = b_d - f_t$) directions. The denominator of Eq. (9) is described in an analogous way. Each of these projection lengths is shown explicitly in *Figure 4*.

Viewing the overlap factors in this way explains why μ_f is always unity—because the projections for both the current and previous tooth passes are the same, that is, $b_{f_1}/b_{f_0} = b_f/b_f = 1$. Such a perspective also shows that μ_d, being equal to $b_{d_1}/b_{d_0} = (b_d - f_t)/b_d$, approaches unity only as the feed approaches zero, as noted earlier. Regarding μ_q, *Figure 4* shows the four general situations that may arise. *Figure 4a* shows a case where μ_q is positive and less than unity. However, when the q direction intersects the free surface between S_0 and S_1, μ_q is negative, as shown in *Figure 4b*. The difference between the positive and negative cases shown is simply a difference in mode orientation, which causes a change in sign from positive to negative in the numerator of μ_q, $b_{f_1}\cos\theta + b_{d_1}\sin\theta$. The extremes of μ_q being infinite and zero are shown in *Figures 4c* and *4d*, respectively. For the cases shown, the change from negative to infinite (from *Figure 4b* to *4c*) results solely from an increase in depth of cut, which causes $b_{f_0}\cos\theta$ to equal $-b_{d_0}\sin\theta$ so that their sum, the denominator of μ_q, becomes zero. For the same depth of cut as in *Figure 4c*, *Figure*

4d shows that a different mode orientation angle causes $b_{f_1}\cos\theta$ to equal $-b_{d_1}\sin\theta$ so that their sum, the numerator of μ_q, becomes zero. When the q direction intersects the free surface to the feed side (left) of S_0, both the numerator and denominator of μ_q become negative, making μ_q positive and greater than unity, becoming unity again when θ reaches π.

Effects of Overlap Factor on Stability Limits

The effect of overlap factor across the traditional range of zero to unity has been studied by others (Nigm 1981, Moriwaki and Iwata 1976, Srinivasan and Nachtigal 1978, Jensen and Shin 1997). Because none have conceived of overlap factors outside that range, the effects of such have not been explored. Here, the effects of nontraditional overlap factor values on stability limit in the spindle-speed domain are explored.

The overlap factor expressions [e.g., Eq. (8)] are strongly dependent on the controllable process inputs of corner radius, lead angle, feed, and mode orientation. However, the overlap factor itself is not controllable. To conduct this study of overlap factor outside its traditional range, in a controlled fashion, the case of straight-edged orthogonal cutting is considered first where overlap factor may be set arbitrarily. Following that, the effects of corner radius, lead angle, feed, and mode orientation are explored with special attention paid to how their overall effects on stability limit are or are not correlated to the overlap factor by tracking overlap factor values along the stability limit boundaries.

Straight-Edged Orthogonal Cutting

The general stability solution form is

$$K_q^2\left(\Re^2+\Im^2\right)\left(1-\mu_q^2\right)-2\Re K_q+1=0 \tag{10}$$

and

$$\varepsilon_c=\tan^{-1}\left(\frac{-\Im}{K_q\left(\Re^2+\Im^2\right)-\Re}\right) \tag{11}$$

where $\Re$ and $\Im$ are the real and imaginary parts of the structure's frequency response function, $G(j\omega)$, evaluated at the chatter frequency ω_c. To illustrate here, second-order dynamics are assumed with stiffness k, damping ratio ζ, and natural frequency ω_n. In Eqs. (10) and (11), $K_q = K_d u_T w$ is the process stiffness, which is the product of a force directional factor K_d, the specific thrust energy u_T, and the width of cut w. So as not to detract from the issue at hand by introducing numeric values for the specific energy, the stability limit (w_{lim}) is presented as $K_{q_{lim}}$ instead. Furthermore, so that specific values of structural parameters need not be introduced, the stability limit is presented in a nondimensional form as $K_q|G(0)|$, where $|G(0)|$ is the zero-frequency (static) magnitude of the frequency response function, that is, the static compliance, which is $1/k$ for the second-order dynamics used here. Finally, the well-known speed axis normalization of tooth frequency by natural frequency, ω_t/ω_n, is used. These various normalizations allow all comparisons to have no dependence on an arbitrary choice of structural dynamics parameters or specific energy values.

A quick observation of Eq. (10) is that overlap factor shows up only in its square. Therefore, both positive and negative values of μ_q that are the same in magnitude will yield identical results. In evaluating the stability equations here, $K_{q_{lim}}$ is computed from Eq. (10) via the quadratic formula and then substituted into Eq. (11) to compute the associated chatter phase. Because the result for $K_{q_{lim}}$ comes from the quadratic formula, results may be positive real, negative real, or complex. Only real-valued results with the same sign as K_d are physically sensible (valid), for only these results yield positive real values for the limiting width of cut. The stability diagram is constructed by incrementing the chatter frequency from zero to four times the natural frequency and keeping only valid results for $K_{q_{lim}}$. The frequency values less than the natural frequency become active when the directional factor is positive or when $|\mu_q| > 1$.

The effect of overlap factor on stability limit is shown in *Figure 5* for $K_d = -1$, which is the usual case of orthogonal cutting where the thrust force acts against the tool vibration into the workpiece. For overlap factors less than unity (*Figure 5a*), as is well known, the stability limit is higher than for unity overlap. The left side of each lobe that asymptotically goes to infinity at ω_t/ω_n = 1/1, 1/2, 1/3, ... for unity overlap, in this case, curves back into the positive speed direction leaving relatively wide and very high "peaks." Based on the phase plots, the downward shift of the stability limit is a

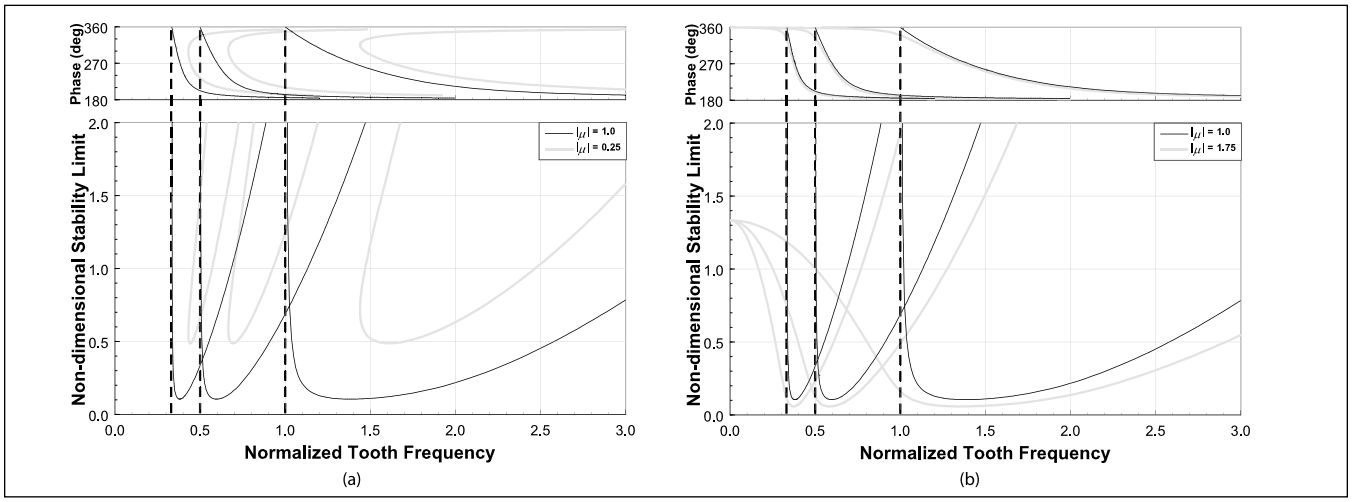

Figure 5
Effect of Overlap Factor on Nondimensional Stability Limit and Chatter Phase for Straight-Edged Orthogonal Cutting at $|\mu_q|$ of: (a) 0.25 and (b) 1.75

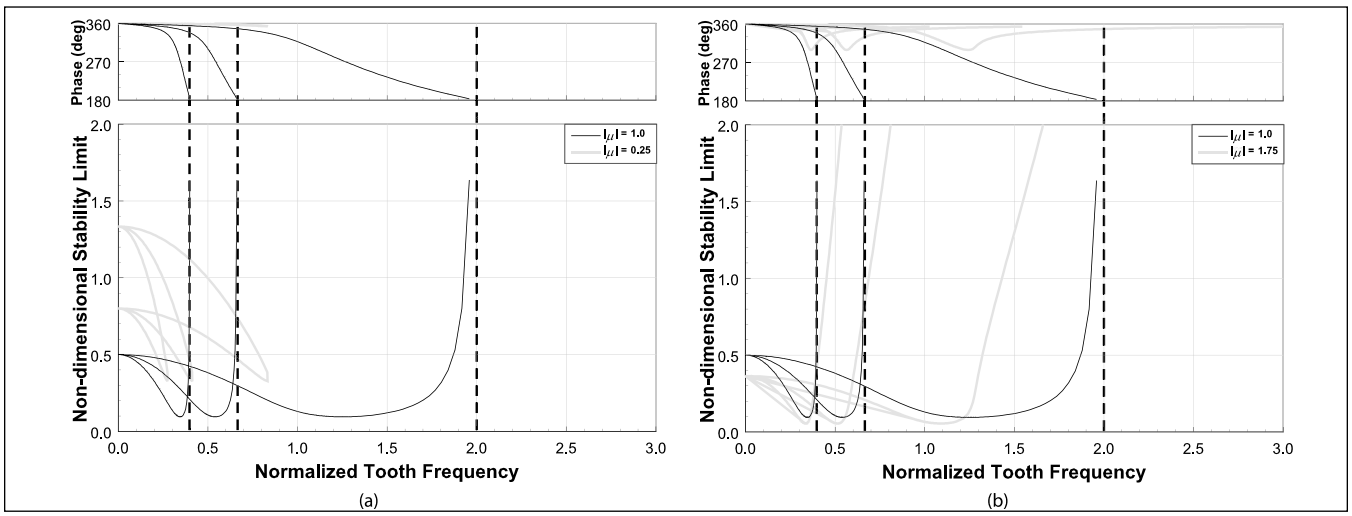

Figure 6
Effect of Overlap Factor on Nondimensional Stability Limit and Chatter Phase for Straight-Edged Orthogonal Cutting, with a Positive Force Directional Factor, at $|\mu_q|$ of: (a) 0.25 and (b) 1.75

result of K_q depending on μ_q, while the change in shape is a result of the phase through its mapping of chatter frequency to the speed domain.

What has not been explored before is the effect of overlap factors with magnitude greater than unity. *Figure 5b* shows a significant effect where all the lobes converge to a single stability limit value at zero speed. The fact that the lobes curve to the left instead of to the right, or vertically as for $|\mu_q| = 1$, means that the peaks are diminished substantially relative to $|\mu_q| = 1$. As one may expect, the tangential limit is reduced as well.

When the directional factor is positive, the results change dramatically, as shown in *Figure 6*. Positive directional factors occur for very large positive rake angles where the thrust force pulls the tooth into the workpiece, or in milling due to the tooth orientation changing with rotation. The geometry introduced by corner radiused tooling may also introduce a positive directional factor. For overlap factor magnitudes less than unity, the stability limit boundaries curve back on themselves instead of asymptotically approaching infinity at the shown unity-overlap asymptotes of ω_t/ω_n = 2/1, 2/3, 2/5, ... This creates only pockets of instability in the union of their interiors. When the overlap factor magnitude is greater than unity, there is not as dramatic a change in the shape of the stability boundaries as was seen for negative directional factors; however, there is a consistent reduction in stability

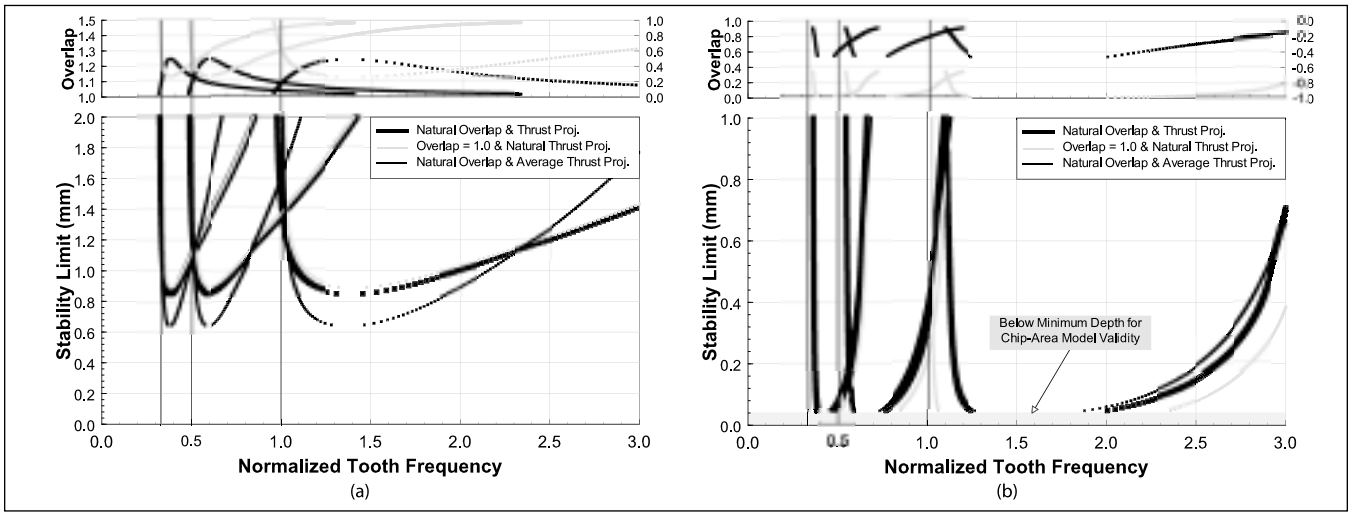

Figure 7
Relative Effects of Overlap Factor and Thrust Force Projection in the *q* Direction for: (a) $\psi = -30°$ and $\theta = 150°$, and (b) $\psi = 30°$ and $\theta = 90°$

limit across all speeds, as compared to $|\mu_q| = 1$. The phase again seems to drive the shape changes; it barely deviates below 360° as $|\mu_q|$ becomes small.

The discussion here must be taken with some caution. Here, it was assumed that the process gain K_q is independent of the overlap factor μ_q. However, the discussion to follow shows that for corner-radiused tools, K_q and μ_q are coupled and, in fact, as $|\mu_q|$ approaches infinity, K_q is approaching zero. Likewise, when $|\mu_q|$ is becoming smaller than unity, K_q is increasing. The question is, are the positive/negative effects of $|\mu_q|$ becoming less/greater than unity offset by the opposite change in K_q?

The Turning Process

The stability equations for turning are, in their general form, the same as those given in Eqs. (10) and (11), where μ_q is as given in Eq. (9) and the process gain is

$$K_q = -\cos(\theta - \bar{\psi})\, u_T (b_f \cos\theta + b_d \sin\theta) \qquad (12)$$

Here, $\bar{\psi}$ is the direction of the modeled process force (thrust force) in the feed-depth plane. The directional factor (K_d) in this case is the product of $-\cos(\theta - \bar{\psi})$ and $(b_f \cos\theta + b_d \sin\theta)$, while the latter term also embodies the measure of width of cut, in this case the depth of cut. The term $(b_f \cos\theta + b_d \sin\theta)$ is also the denominator of μ_q [see Eq. (9)]. Therefore, the right-hand side of the equation of motion (the dynamic process force ΔF_q), and its representation in overlap factor form, evolves as

$$\begin{aligned}
\Delta F_q &= -\cos(\theta - \bar{\psi})\, u_T \Delta a(t) \\
&= -\cos(\theta - \bar{\psi})\, u_T \left[(b_f \cos\theta + b_d \sin\theta) q(t) \right. \\
&\qquad \left. -(b_f \cos\theta + (b_d - f_t)\sin\theta)\, q(t - T_t)\right] \\
&= -\cos(\theta - \bar{\psi})\, u_T (b_f \cos\theta + b_d \sin\theta)\left[q(t) - \mu_q q(t - T_t)\right] \\
&= K_q \left[q(t) - \mu_q q(t - T_t)\right]
\end{aligned}$$

From these relations, it is clear that K_q and μ_q [see Eq. (9)] are coupled through each being a function of depth of cut (the usual measure of stability, a dependent variable of the analysis), as is any model of $\bar{\psi}$. As a result, it is impossible to look at a normalized stability limit of a form like $K_d u_T w|G(0)|$ as was done for the orthogonal cutting case. Therefore, the traditional stability limit measure of limiting depth of cut, d_{lim}, is studied here. The computation of stability limits here is done in the same way as was described in the previous work that presented the turning stability solution (Ozdoganlar and Endres 1998). The structural dynamics and process force model coefficients from that work are used here with a corner radius of 0.8 mm (1/32 inch) and a feed of 0.15 mm (0.006 inch).

Figure 7 shows two examples of computed stability limits and (in the upper plot) the associated overlap factor and thrust force projection onto the *q*-direction. The thrust force projection is the term $-\cos(\theta - \bar{\psi})$. Each stability diagram shows the "natural" prediction, in which case both μ_q and $\bar{\psi}$ (i.e., the thrust projection) are allowed to vary naturally

with their dependence on depth of cut—the stability limit. Also shown is the result for when the overlap factor is constrained to unity as well as when the thrust force projection is constrained to be constant at its average value of the "natural" result. If the constant thrust projection case deviates more from the "natural" case than does the $\mu_q = 1$ case, this indicates that the variation in overlap factor and its deviation from unity is masked by the other process geometry effects in K_q, specifically the equivalent lead angle $\overline{\psi}$ changing with depth of cut. This is the case in *Figure 7a*. *Figure 7b* shows that, in other cases, variation in overlap factor and its deviation from unity does indeed affect the results, dominating the effects of K_q and $\overline{\psi}$, even in light of the complicated coupling between μ_q and K_q.

The only conclusion that may be drawn is that the interactions among μ_q and K_q through depth of cut are complicated and vary significantly with other process variables such as lead angle and mode orientation. This means that the traditional notion of overlap factor being the mathematical remedy for generalizing the stability problem must be considered with great caution because in real processes, such as those with corner-radiused tools, overlap factor (1) is not just a number and (2) is tightly coupled to other aspects of the problem.

Conclusions

The conclusions from this study are as follows:

- Overlap factor is not simply a number; it is mathematically dependent on process parameters, including the depth of cut, which is the usual dependent variable of a stability solution.
- When using corner-radiused tooling, the overlap factor can mathematically take on any value, not only those between zero and unity.
- The trends seen when varying the overlap factor in a straight-edged orthogonal analysis must be considered with caution, as corner-radiused process geometry involves directional issues as well, which in some cases mask the effects of overlap factor variation across the stability diagram.
- It seems unlikely that extreme overlap values toward infinity would ever occur because there is strong dependence on depth of cut, which is the solution result in stability analysis, not a set value.
- To assess stability of corner-radiused processes, one must resort to the complete solution, not qualitative overlap-based assessments.

Acknowledgments

The authors wish to gratefully acknowledge the financial support of the ERC for Reconfigurable Machining Systems under NSF grant EEC-9529125, as well as the participation of our industry participants, including Caterpillar, Cummins, Ford, General Motors, and Lamb Technicon.

References

Gurney, J.P. and Tobias, S.A. (1961). "A graphical method for the determination of the dynamic stability of machine tools." *Int'l Journal of Machine Tool Design Research* (v1), pp148-156.

Jensen, A.S. and Shin, Y.C. (1997). "Stability analysis in face milling operations: Part 1—Theory of stability lobe prediction; Part 2—Experimental validation and influencing factors." *ASME Journal of Mfg. Science and Technology* (MED 6-2), pp403-418.

Merchant, M.E. (1944). "Basic mechanics of metal cutting process." *Journal of Applied Physics* (v66), pp. A168-A175.

Merritt (1965). "Theory of self-excited machine-tool chatter: Contribution to machine tool chatter research—1." *ASME Journal of Engg. for Industry* (v87), pp447-454.

Moriwaki, T. and Iwata, K. (1976). "In-process analysis of machine tool structure dynamics and prediction of machining chatter." *ASME Journal of Engg. for Industry* (v98), pp301-305.

Nigm, M.M. (1981). "Experimental investigation of the characteristics of dynamic cutting processes." *Int'l Journal of Machine Tool Design Research* (v21), pp251-261.

Ozdoganlar, O.B. and Endres, W.J. (1998). "An analytical stability solution for the turning process with depth-direction dynamics and corner-radiused tooling." *Proc.* of Symp. on Advances in Modeling, Monitoring, and Control of Machining Systems, ASME IMECE (DSC-64), pp511-518.

Ozdoganlar, O.B. and Endres, W.J. (2000). "An analytical representation of chip area for corner-radiused tools under depth-of-cut and feed variations." *ASME Journal of Mfg. Science and Engg.* (v122), pp660-665.

Srinivasan, K. and Nachtigal, C.L. (1978). "Investigation of the cutting process dynamics in turning operations." *ASME Journal of Engg. for Industry* (v100), pp323-331.

Sweeney, G. and Tobias, S.A. (1969). "Survey of basic machine tool chatter research." *Int'l Journal of Machine Tool Design Research* (v9), pp217-238.

Tobias, S.A. and Fishwick, W. (1958). "The chatter of lathe tools under orthogonal cutting conditions." *Trans. of ASME* (v80), pp1079-1088.

Authors' Biographies

Dr. William J. Endres is an associate professor in the Dept. of Mechanical Engineering-Engineering Mechanics at Michigan Technological University. He received his BS (1988), MS (1990), and PhD (1992) degrees in mechanical engineering from the University of Illinois at Urbana-Champaign. His research interests include machining dynamics, cutting mechanics, and mechanistic modeling techniques with an emphasis on the effects of edge bluntness, wear-land geometry, and other cutting tool geometry on the evolution of process performance, including dimensional accuracy, surface waviness (vibration), surface finish, residual stresses, and stability/chatter.

Dr. O. Burak Ozdoganlar is a senior member of the technical staff in the Structural Dynamics and Smart Systems organization at Sandia National Laboratories. He received his BS (1991) in aerospace engineering from Istanbul Technical University (Turkey), MS (1993) in aerospace engineering and MS (1995) in mechanical engineering from Ohio State University, and PhD (1999) in mechanical engineering from the University of Michigan. His research interests include manufacturing processes and systems, specifically machine tool dynamics, machining process modeling, machining dynamics and chatter, process planning, and intelligent fixturing. His recent interests also include dynamic modeling and testing and analysis of microsystems (MEMS).